ELSEVIER

Journal of Marine Systems 36 (2002) 75–100

JOURNAL OF MARINE SYSTEMS

www.elsevier.com/locate/jmarsys

An Ensemble Kalman filter with a 1-D marine ecosystem model

Mette Eknes *, Geir Evensen

Nansen Environmental and Remote Sensing Center, Edvard Griegsvei 3a, N-5037 Solheimsviken Bergen, Norway

Received 1 December 1999; accepted 7 March 2002

Abstract

The Ensemble Kalman Filter (EnKF) has been examined in a data assimilation experiment with a one-dimensional three-component ecosystem model. The model is an extension of the zero-dimensional model developed by Evans and Parslow [Biol. Oceanogr. 3 (1985) 327.]. The purpose of this paper is to examine the possibilities of using a sequential data assimilation method for state estimation in a biological model, an approach which differs from the more traditional parameter estimation studies. The method chosen is the Ensemble Kalman Filer (EnKF), and it has been shown that this method captures the nonlinear error evolution in time and is capable of both tracking the reference solution and to provide realistic error estimates for the estimated state. This is an indication that the methodology might be suitable for future operational data assimilation systems using more complex three-dimensional models. © 2002 Elsevier Science B.V. All rights reserved.

Keywords: Ensemble Kalman filter; 1-D marine ecosystem model; Data assimilation experiment

1. Introduction

There is now a strong international focus on development of data assimilation systems for biological models. The purposes of these studies have so far been twofold. A number of papers have considered the use of data assimilation techniques for estimating poorly known parameters in the models, e.g. Ishizaka (1993), Spitz et al. (1998), Lawson et al. (1995, 1996), Prunet et al. (1996a,b), Fasham and Evans (1995), Matear (1995), Hurtt and Armstrong (1996). This is obviously a very important issue since many of the model parameters are far from empirical and need to be calibrated both through laboratory experiments and by trial and error in the open ocean. A few related references to parameter identification problems in physical oceanography are the papers by Smedstad and O'Brien (1991), Yu and O'Brien (1991, 1992) and Eknes and Evensen (1997). See also Evensen et al. (1998) which reviews the formulation of the parameter estimation problem, and Navon (1997) which provides a number of links to parameter estimation problems solved in other scientific fields.

Another application of data assimilation which has become popular and useful in physical oceanography and meteorology is related to state estimation. Thus, one considers the problem of estimating the model state over some time period by simultaneously extracting a maximum amount of information out of

* Corresponding author. Tel.: +47-55-297288; fax: +47-55-200050.

E-mail addresses: Mette.Eknes@nersc.no (M. Eknes), Geir.Evensen@nersc.no (G. Evensen).

0924-7963/02/$ - see front matter © 2002 Elsevier Science B.V. All rights reserved.
PII: S0924-7963(02)00134-3

a dynamical model and a set of observations. Data assimilation methods have now been developed for state estimation both in physical oceanography and meteorology for use in operational forecasting and monitoring systems. Recently, the focus has also turned towards biological state estimation, for developing coupled biological and physical data assimilation systems, which can be used for operational forecasting of the coastal marine ecosystem. The number of publications and applications of data assimilation in physical oceanography is huge, and there are several established techniques being used with models of different complexity. A comprehensive review of data assimilation methods is not possible here, but one can differentiate between methods traditionally implemented for linear model dynamics, e.g. the Kalman Filter, see Kalman (1960) and Kalman and Bucy (1961) for the original works, and the adjoint technique first properly introduced to oceanography and meteorology by Talagrand and Courtier (1987) and Courtier and Talagrand (1987). These techniques have later been further developed and extended to work with nonlinear model dynamics with variable success. For example, the Extended Kalman Filter applies a linearization for the error covariance evolution which may become unstable for some problems (Evensen, 1992), and a similar problem applies for the adjoint method since a tangent linear approximation constrains the length of the assimilation time interval which can be used (Miller et al., 1994).

On the other hand, there has also been a significant development of new assimilation formulations and techniques which have been tailored to work with nonlinear dynamical models. One such method, the Ensemble Kalman Filter (EnKF), is used in this study. The method has been chosen based on its properties for predicting error statistics for strongly nonlinear systems, see Evensen (1994, 1997), and for its simplicity and numerical efficiency.

The model parameters will be kept fixed with predefined values. Thus, the model serves as a non-perfect estimate of the true evolution of the biological system (in some statistical sense), and thus contains errors which are allowed for in the EnKF. Only the prognostic variables, i.e. concentrations of the nutrient, phytoplankton and herbivorous zooplankton, will be estimated. This is as far as we know only the third paper discussing state estimation in biological models using data assimilation. The first paper was the one by Natvik et al. (2001) where a weak constraint inverse method was used with the original zero-dimensional model by Evans and Parslow (1985), and the second is a recent application by Carmillet et al. (2001).

In this paper, a three-component one-dimensional extension of the zero-dimensional ecosystem model by Evans and Parslow (1985) will be used in data assimilation experiments. In the following sections, the ecosystem model is described and then the EnKF is briefly explained.

We then present results from twin experiments where simulated data are used in assimilation experiments. Finally, a sensitivity analysis regarding the levels of model and measurement errors is performed.

2. The model

Evans and Parslow (1985) investigated the biological features in the ocean common to annual cycles, in particular, spring blooms. For this purpose, they constructed a fairly simple differential equation model of nutrients, phytoplankton and herbivores in a mixed layer of varying depth, i.e. responding to physical changes which have the same pattern from year to year. The response of phytoplankton to light was modeled in some detail, while other aspects were less detailed.

Here, this model has been further extended to contain a vertical dimension in addition to the time dimension. This was done by replacing the terms including diffusion rate (m in the original equations) for the concentrations of nutrients, phytoplankton and zooplankton, with a vertical diffusion term parameterized on the form $(\partial/\partial z)(K_z(z, M)(\partial/\partial z))$, where K_z is a diffusion coefficient. The mixed layer depth M is used as a physical input to the ecosystem model. As in Natvik et al. (2001), a smooth version of the mixed layer depth function $M=M(t)$ is used together with second order finite difference formulas to estimate the rate of change of the mixed layer depth M. A plot of the mixed layer depth function is given in the upper left plot in Fig. 3 where the reference solution for the concentration of nutrients is also shown.

The model equations describing the time evolution for nutrients, N, phytoplankton, P, and herbivores, H, are given by

$$\frac{\partial N}{\partial t} = -\left[\frac{\alpha(t,z,P)N}{j+N} - r\right]P + \frac{\partial}{\partial z}\left(K_z(z,M(t))\frac{\partial N}{\partial z}\right), \tag{1}$$

$$\frac{\partial P}{\partial t} = \left[\frac{\alpha(t,z,P)N}{j+N} - r\right]P - \frac{c(P-P_0)H}{K+P-P_0} + \frac{\partial}{\partial z}\left(K_z(z,M(t))\frac{\partial P}{\partial z}\right), \tag{2}$$

$$\frac{\partial H}{\partial t} = \frac{fc(P-P_0)H}{K+P-P_0} - gH + \frac{\partial}{\partial z}\left(K_z(z,M(t))\frac{\partial H}{\partial z}\right). \tag{3}$$

The depth dependent diffusion parameter, K_z, is given by

$$K_z(z,M(t)) = K_{z_b} + \frac{(K_{z_0}-K_{z_b})(\operatorname{atan}(\gamma(M(t)-z)) - \operatorname{atan}(\gamma(M(t)-D)))}{\operatorname{atan}(\gamma M(t)) - \operatorname{atan}(\gamma(M(t)-D))}, \tag{4}$$

where $K_{z_b}=8.64$ (m^2/day) and $K_{z_0}=864.0$ (m^2/day) are the diffusion at the bottom and surface, respectively, $\gamma=0.1$ m^{-1} is the thermocline sharpness, D is the total depth, and the rest of the variables and parameters have the same meaning as in Evans and Parslow (1985), i.e. they are appropriate to Flemish Cap (an offshore bank east of Newfoundland) as in Evans and Parslow (1985) (Table 1). Note, however, that the photosynthetic light rate, α, is defined as in Evans and Parslow (1985) and Natvik et al. (2001), but instead of averaging it over the mixed layer depth, it is now evaluated at the depths where it is needed (see Appendix A). This is the reason why it is no longer dependent on the mixed layer depth M, but just of the phytoplankton concentration, time and depth.

The nutrient concentration at 200 m is kept constant all through the year and serves as an infinite pool of nutrients which are mixed into the biologically active mixed layer by the vertical mixing term. The concentrations of phytoplankton and herbivorous zooplankton are both set equal to zero at 200 m and no flux at the surface has been specified.

Table 1
Physical parameters, appropriate to Flemish Cap, used in the data assimilation experiments for the one-dimensional ecosystem model

Symbol	Description	Value
c	Maximum grazing rate	1.0 day^{-1}
f	Grazing efficiency	0.5
g	Loss to carnivores	0.07 day^{-1}
j	Uptake half saturation	0.5 mmol N m^{-3}
r	Plant metabolic loss	0.07 day^{-1}
K	Grazing half saturation	1.0 mmol N m^{-3}
P_0	Grazing threshold	0.1 mmol N m^{-3}

These are the same parameters as used by Evans and Parslow (1985).

3. The Ensemble Kalman filter formulation

The data assimilation method adopted in this work is the Ensemble Kalman Filter (EnKF) method first introduced by Evensen (1994). The method was formulated with nonlinear dynamics in mind, and the emphasis was focused on deriving a method, which properly could handle the error covariance evolution in nonlinear models. The method has been used successfully with a number of different dynamical models, from the simple but highly nonlinear and chaotic Lorenz equations in Evensen and Fario (1997), to ocean circulation models by Evensen and van Leeuwen (1996) and Evensen (1997). In the EnKF, the errors are dominated by statistical noise and there are no closure problems or unbounded error variance growth as have been seen in assimilation methods relying on the use of a tangent linear model.

The EnKF integrates an ensemble of model states forward in time using the model equations. Normally, the number of members (or samples) is of order 100. If each individual member is integrated as a stochastic differential equation, i.e. forced with a random noise component which represents the model errors, it can be shown that such an ensemble integration becomes identical to a Markov Chain Monte Carlo (MCMC) method for solving the Fokker Planck equation for the evolution in time of the probability density of the model state. Since the full nonlinear dynamical model is used, the only approximation associated with this

approach is that a finite number of members are used in the ensemble.

The ensemble is integrated forward in time until measurements are available. At these time instants, an analysis scheme is used to update or correct the model state in a statistically consistent way. The updated state can be considered as the model forecast plus a number of influence functions, one for each of the measurements. These functions are multivariate statistical functions computed from the ensemble statistics, i.e. the cross-correlations between the different variables in the model are included. Thus, a change in one of the model variables will influence the other variables. This analysis minimizes the error variance of the analyzed estimate in a least square sense, and it is based on estimates of the error statistics for the model forecast and the measurements.

A particularly useful property of the EnKF is that the analysis is repeated for each of the members in the ensemble, and the resulting analyzed ensemble then

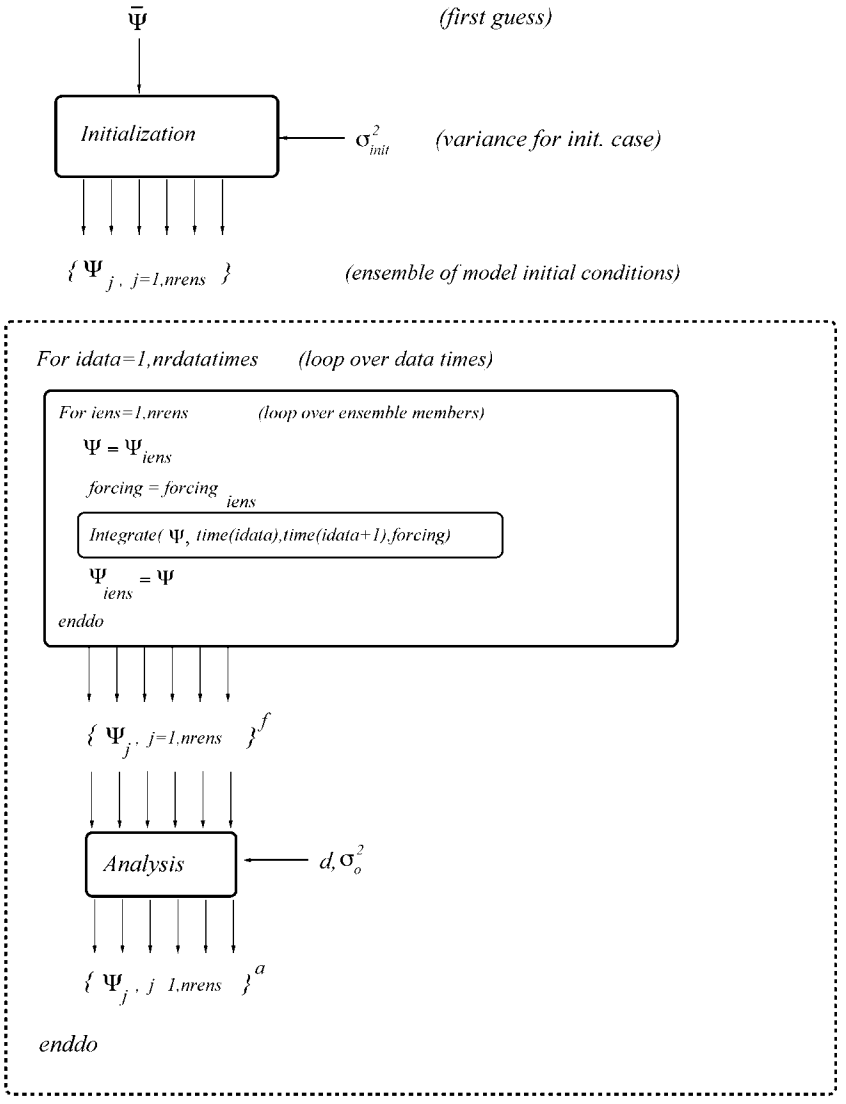

Fig. 1. Schematic figure showing how the EnKF works in relationship with an arbitrary model. See description in text.

has the correct error statistics for the analyzed state. Thus, there is no need for resampling to create a new ensemble for the continuing integration. A detailed presentation of the EnKF implementation is given in Burgers et al. (1998).

A schematic illustration of the algorithm is given in Fig. 1. The figure defines three boxes, i.e. the Initialization box, the Integration box and the Analysis box. The Initialization box takes the first guess model state as input and creates an ensemble of size nrens by adding pseudo random noise with prescribed statistics to the first guess initial state. Each of these perturbed model states is integrated forward in time until the time when the first observation set becomes available. This is done by calling the Integration box which integrates one model state forward in time over a specified time interval. Then each of the members is input to the Analysis box, which computes a new ensemble of analyzed model states based on the ensemble statistics and the observations and their error statistics. The analyzed ensemble is then integrated forward to the next data time and the process is repeated. The EnKF estimate is usually defined to be the ensemble mean.

By use of object-oriented programming, a generic EnKF has been developed. Thus, one has to specify an object which defines a full model state and a subroutine for the model integration and most models can be included in the generic implementation, since the analysis scheme operates on objects of full model states.

4. Experiments

Several so-called twin experiments will now be discussed. A twin experiment is just a notation for data assimilation experiments where the data are simulated using the model rather than using real data. The only reason for using simulated data is to examine the properties of the assimilation methodology. The motivation is that unless the method works fine in the twin experiment, there is no point using it with real data, and besides, it allows the method to be examined in a controlled experiment where all the error statistics are known.

First, the spinup solution, the reference solution, the generation of measurements and a special run called the climatology will be described. Then the two main assimilation experiments are discussed. These assimilation experiments both start from the same initial ensemble as in the climatology simulation and the simulated observations are now used to update the model state sequentially in time using the EnKF.

In all the experiments, the total integration time is 365 days. The total depth of the water column is set to 200 m and the resolution in time and depth is 1 day and 10 m, respectively. The number of ensemble members for these cases is 100, and the boundary and initial errors are given in Table 2.

4.1. Spinup solution

The experiment has been set up as follows: first the model is spun up during a 5-year simulation (see Fig. 2 where the spinup for the nutrient concentration is shown), starting from initial values of $N(z)=10.0$ mmol N m^{-3}, $P(z)=0.1$ mmol N m^{-3} and $H(z)=0.1$ mmol N m^{-3} in the whole water column. The solution after 5 years has reached a nearly steady annual cycle and is considered to be one realization out of a large number of possible model solutions.

4.2. Reference solution

The reference model trajectory, the "true" state, is defined by choosing one of the initial ensemble members (to be defined in Section 4.4) and integrating

Table 2
The variances used in the climatology and the main data assimilation experiments

Description	N	P	H
Model error variance ((mmol N m^{-3}/day)^2)	3.64×10^{-5}	6.04×10^{-8}	1.91×10^{-8}
Initial error variance ((mmol N m^{-3})^2)	1.0×10^{-2}	1.0×10^{-6}	1.0×10^{-6}
Upper boundary error variance ((mmol N m^{-3})^2)	1.0×10^{-4}	1.0×10^{-4}	1.0×10^{-4}
Lower boundary error variance ((mmol N m^{-3})^2)	1.0×10^{-2}	1.0×10^{-4}	1.0×10^{-4}
Measurement error variance ((mmol N m^{-3})^2)	0.33×10^{1}	5.44×10^{-3}	1.72×10^{-3}

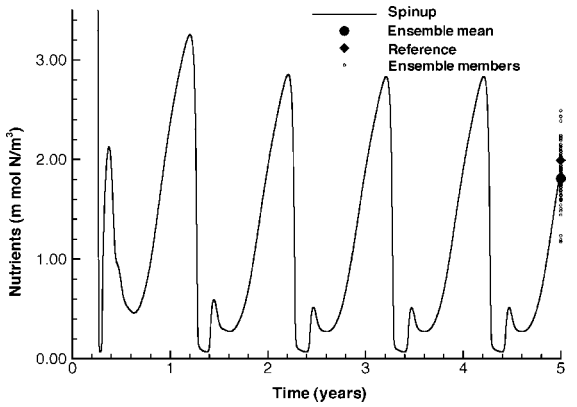

Fig. 2. The spinup simulation for the concentration of nutrients, N, at the surface. The total spinup time is 5 years, and at the end, the initial reference and mean estimates together with the initially generated ensemble are shown.

it forward 1 year. The initial value for the concentration of nutrient for the reference solution is shown in Fig. 2.

Note that a stochastic model error is added at every time step to account for the uncertainty in the model equations, i.e. we are actually integrating the system

$$\frac{\partial \psi}{\partial t} = \boldsymbol{F}(\psi) + \boldsymbol{q}, \tag{5}$$

where $\psi(z,t)=(N(z,t), P(z,t), H(z,t))$, $\boldsymbol{F}$ is the right hand side of Eqs. (1)–(3) and $\boldsymbol{q}(z,t)$ is the stochastic error term (further details are given in Appendix C).

The reference solution is plotted as the left column of Fig. 3. In the upper plot, we have also included the mixed layer depth as a function of time. The phytoplankton concentration is at its highest in the period between 100 and 160 days (i.e. April to June). This is the period where there is a phytoplankton spring bloom. These results are similar to what was found by Evans and Parslow (1985) using the zero-dimensional version of the model. The largest bloom is in the upper 50 m, but there is an obvious bloom in all of the upper 100 m.

There is a depletion of nutrient concentration during the phytoplankton bloom and it only starts recovering after the phytoplankton concentration has decreased, but it is still low until day 300 in the upper 100 m, which is the time when the winter deepening of the mixed layer starts and leads to entrainment of nutrients from below the mixed layer.

The bottom plot in Fig. 3 shows the concentration of herbivorous zooplankton. It has its largest value in the period from about days 150 to 175 when the phytoplankton bloom is ending. As the concentration of zooplankton is increasing, there is enhanced grazing on the phytoplankton biomass until it has nearly vanished and the zooplankton begins to die and the concentration decreases to about the level it had before the bloom.

4.3. Simulation of measurements

The simulated observations are generated by measuring the reference solution and then adding independent Gaussian noise with zero mean and a prescribed variance to the observations.

Measurements were generated every 4th day at 20-, 60-, 100- and 140-m depth. For Experiment 1 (Case 1A in Table 3), all three components of the model state are observed, and thus, there is a total of 12 measurements at each of 121 different times over 1 year. For Experiment 2 (Case 5C in Table 3), only the phytoplankton variable is observed, and thus, the corresponding number at each of the measurement times is 4. The measurement errors for the different experiments are explained in Table 3.

4.4. Generation of the initial ensemble

For the assimilation experiment, we generated a new initial condition by adding another pseudo random field to the spinup solution. This was then considered to be our "best guess estimate" of the truth (see Fig. 2). The same initial variance for the initial condition as in the reference case was used.

An ensemble of model states was then generated by adding pseudo random fields to the "best guess estimate". Again, the statistics is the same as for the reference solution, and the mean of the ensemble equals the best guess estimate. The covariance in depth has been treated as in Evensen (1994).

Some of the ensemble members for the nutrient concentration N used initially are shown in Fig. 2. Note that, in fact, any of these ensemble members could have been used to generate a reference solution for the twin experiments.

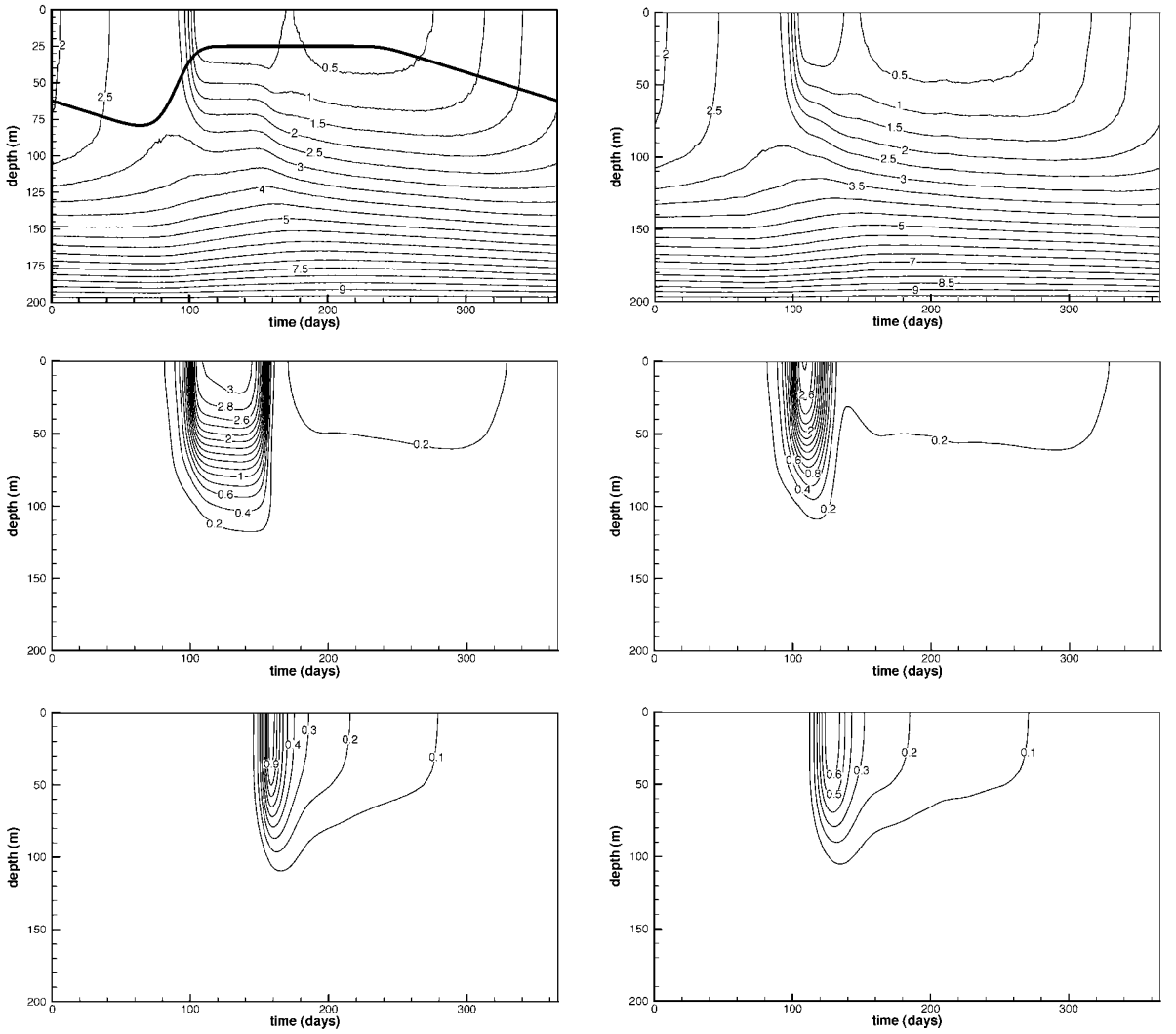

Fig. 3. The reference (left) and the climatology (right) solutions of the concentration of the nutrient N (top), the phytoplankton P (middle) and the zooplankton H (bottom), respectively. The mixed layer depth is shown as the thick solid line in the upper left plot. All variables are presented in mmol N m^{-3}.

4.5. Climatology

A statistical climatology can be generated by a pure ensemble simulation with no influence from the data. The ensemble is integrated forward in time for 1 year and the resulting ensemble mean is denoted the climatology. The spreading of the ensemble members around this mean determines the variance or uncertainty in the climatology. The climatology solution is shown in the right column of Fig. 3, and it clearly deviates from the reference solution. The phytoplankton concentration is lower, since each of the ensemble members is blooming at slightly different times and the averaging of the ensemble smoothens out the peaks in time. However, it should be noted that even if the result is far from the reference solution, this is also represented well by the error estimate from the ensemble statistics, which will be discussed in connection with the assimilation experiments.

Table 3
The errors, ensemble sizes (nrsamp) and residual root mean squares (resRMStds) of N, P and H in the different twin experiments

Experiments	Observation	$\mathrm{Std}_{\mathrm{obs}}$ (%)	$\mathrm{Std}_{\mathrm{mod}}$ (%)	nrsamp	$\mathrm{resRMStd}_N$	$\mathrm{resRMStd}_P$	$\mathrm{resRMStd}_H$
Case 1A	NPH	30	1.0	100	1.23e − 1	4.17e − 2	2.06e − 2
Case 1B	NPH	30	1.0	70	1.43e − 1	3.87e − 2	2.08e − 2
Case 1D	NPH	30	1.0	40	1.44e − 1	4.58e − 2	2.21e − 2
Case 1E	NPH	30	1.0	10	1.86e − 1	6.47e − 2	2.79e − 2
Case 1F	NPH	30	1.0	120	1.28e − 1	3.93e − 2	2.03e − 2
Case 1G	NPH	30	1.0	150	1.33e − 1	4.03e − 2	2.08e − 2
Case 1H	NPH	30	1.0	1000	1.27e − 1	4.01e − 2	2.02e − 2
Case 2A	NPH	30	3	100	2.67e − 1	3.01e − 2	3.50e − 2
Case 2B	NPH	1	3	100	6.32e − 2	1.07e − 2	7.82e − 3
Case 3A	N	1	3	100	8.18e − 2	4.49e − 1	1.38e − 1
Case 3B	N	1	1	100	5.94e − 2	3.56e − 1	1.33e − 1
Case 3C	N	30	1	100	1.40e − 1	4.17e − 1	1.11e − 1
Case 4A	P	1	3	100	1.30e − 1	7.33e − 3	7.47e − 3
Case 4B	P	1	1	100	4.93e − 2	3.22e − 3	2.77e − 3
Case 4C	P	30	1	100	9.81e − 2	2.13e − 2	1.52e − 2
Case 5A	H	1	3	100	5.24e − 1	3.13e − 1	2.78e − 3
Case 5B	H	1	1	100	1.61e − 1	1.24e − 1	1.58e − 3
Case 5C	H	30	1	100	1.38e − 1	1.43e − 1	1.26e − 2
Case 6A (nB)	NPH	1	1	100	1.05e − 1	4.04e − 1	9.58e − 2
Case 6B (oB)	NPH	1	1	100	2.73e − 2	3.77e − 3	2.94e − 3

The resRMStd refers to the fact that the resRMS has been averaged over time and depth domain. It is calculated for each of the three state variables and says something about the distance (time mean distance) between the "true" reference solution and the EnKF estimate. The standard deviation of the errors in the model dynamics ($\mathrm{Std}_{\mathrm{mod}}$) and the standard deviation of the errors in the observations ($\mathrm{Std}_{\mathrm{obs}}$) are given as certain percentages of the time and depth mean of the reference solution (taken over 1 year) and the observations used, respectively. The corresponding variances are the squares of the numbers found by calculating these percentages. Note that measurements from the bloom period only (oB = onlyBloom) have been assimilated in Case 6A, while measurements from the pre- and post-period of the spring bloom period (nB = noBloom) have been assimilated in Case 6B.

The spreading of the ensemble around the mean, i.e. the variance, provides an estimate of the uncertainty of the mean as a function of time. The climatology run is made in order to be able to examine the impact of the assimilation of data, by comparing the EnKF estimate with the climatology run. A more realistic estimate will now be found by including the information contained in the measurements.

4.6. Error measures

When discussing twin experiments, it is possible to compute a measure of the distance between the EnKF estimate and the reference case which is referred to as the residual root mean (in depth) square, hereafter denoted resRMS. It is defined as

$$\mathrm{resRMS} = \sqrt{\frac{1}{kdim}\sum_{i=1}^{kdim}(\psi_i^{\mathrm{ref}} - \psi_i^{\mathrm{est}})^T(\psi_i^{\mathrm{ref}} - \psi_i^{\mathrm{est}})}, \tag{6}$$

where $kdim$ is the total number of grid points in depth, while the vectors ψ^{ref} and ψ^{est} holds the reference solution and the EnKF (or climatology) estimate on this grid.

The corresponding residual over the time and depth domain is computed as

$$\mathrm{resRMStd} = \sqrt{\frac{1}{kdim}\frac{1}{ndim}\sum_{i=1}^{kdim}\sum_{j=1}^{ndim}(\psi_{i,j}^{\mathrm{ref}} - \psi_{i,j}^{\mathrm{est}})^T(\psi_{i,j}^{\mathrm{ref}} - \psi_{i,j}^{\mathrm{est}})}, \tag{7}$$

where $ndim$ is the total number of grid points in time.

The EnKF provides a statistical error estimate which can be compared with the absolute value of the residual between the reference solution and the current estimate. To be able to compare with the

resRMS, we define the ensemble root mean (in depth) square (ensRMS) by

$$\text{ensRMS} = \sqrt{\frac{1}{kdim}\sum_{i=1}^{kdim}\sigma_i^2}, \tag{8}$$

where σ^2 is the error variance provided by the EnKF.

If the analysis is done properly, the predicted ersRMS and actual resRMS values should be of the same order of magnitude.

Clearly, a large number of assimilation experiments should be used to get a statistical intercomparison between the estimated and true errors. In this case, we only consider one simulation and expect the true errors to be "similar" to the estimated ones. This turns out to be the case in the experiments presented below where the absolute values of the residuals are of the same magnitude as the estimated errors, although slightly lower.

4.7. Experiment 1: Observing all the three ecosystem components

In this experiment, referred to as Case 1A in Table 3, data from all the three ecosystem variables are assimilated. The resulting EnKF estimate is shown in Fig. 4. What is seen by comparing this estimate with the reference solution (Fig. 3) is that we now seem to have a more realistic estimate of all the three components compared to the climatology simulation. The phytoplankton spring bloom occurs at the same time and has approximately the same magnitude as in the reference solution, and the other two components are also very similar to the corresponding components of the reference solution. Note the discontinuities in time, at the measurement times, which is a characteristic of sequential assimilation methods.

For the concentrations of phytoplankton and herbivorous zooplankton, both of them have the largest errors during the spring bloom (i.e. around days 100–160). This is due to the fact that the model is the most unstable in this periods (see Appendix B).

For the nutrient concentration, the largest error is around day 90, at the time when the spring bloom starts, but the values are otherwise oscillating around 0.0075, i.e. they are at about the same level throughout the whole year.

4.8. Experiment 2: Observing P only

This experiment, which corresponds to Case 4C in Table 3, is similar to Experiment 1, except that only phytoplankton observations are assimilated. The resulting estimate is shown in Fig. 5. Clearly, the phytoplankton observations are sufficient to control the whole model state including nutrients and zooplankton. Thus, the multivariate statistical influence functions are used to update both the observed variable and the two other model variables simultaneously. For future studies, it would be interesting to examine how complicated models can be and still be controlled by the EnKF when measurements of only one or a few of the model variables are available.

When comparing the results between Experiments 1 and 2, the model solutions are very similar, and also close to the reference solution. However, one would expect the estimated standard deviations and absolute values of the residuals to be larger in Experiment 2 since less information is assimilated. This is true for the nutrients, but for the phytoplankton and zooplankton, the resRMSs are of about the same magnitude.

The observed phytoplankton variable is better controlled than the two others, but there is also a strong effect from the observations on the nutrients, N, and the herbivorous zooplankton, H. This is seen in particular during the spring bloom where the phytoplankton data also provides a strong update of the zooplankton.

4.9. Discussion

The resRMSs for the climatology, Experiments 1 and 2, are shown in Fig. 6. In the climatology case, the resRMSs for all the three components are quite small until about day 100 when it starts increasing. While the resRMS for the nutrient reaches a maximum value at about day 150, the resRMS for the concentration of phytoplankton reaches its maxima about at day 140. The resRMS for the concentration of zooplankton, however, has two peaks, one around day 120 and another at about day 160. This is in the spring bloom period where the model is the most unstable (see Appendix B), and the errors therefore are the largest. After the phytoplankton spring bloom period, at about day 170, the resRMSs for the phytoplankton

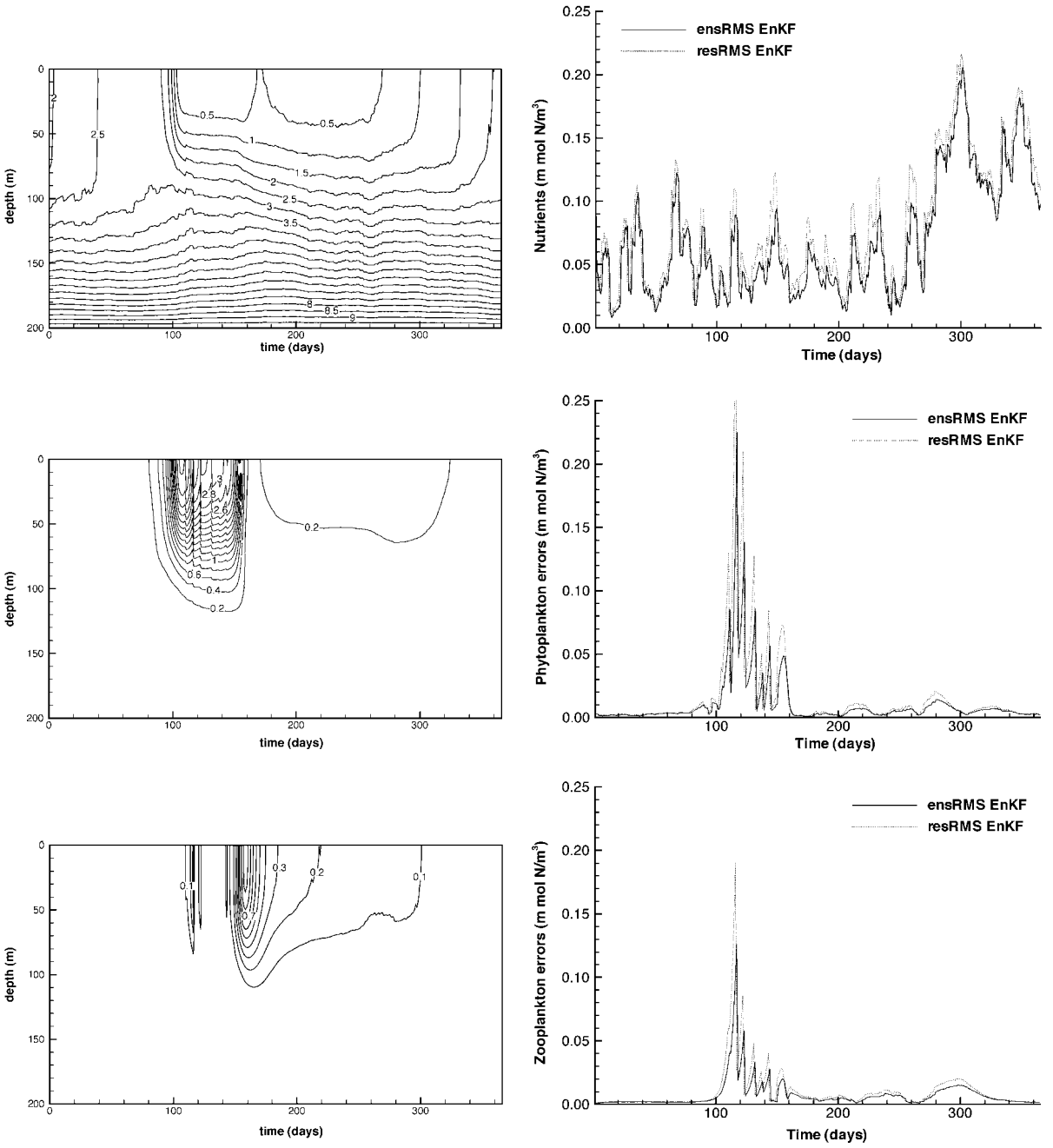

Fig. 4. Experiment 1 (Case 1A): The EnKF estimate (left plots) and comparison of the corresponding resRMS and ensRMS measures (right plots), for nutrient N (upper), phytoplankton P (center) and herbivorous zooplankton H (lower).

concentration have decreased to about the same level as before the spring bloom. For the concentrations of nutrient and zooplankton, the resRMS levels from the pre-bloom period are not reached before until about day 300. In the case of the nutrients, this is mostly due to a high variance below the mixed layer, which is not

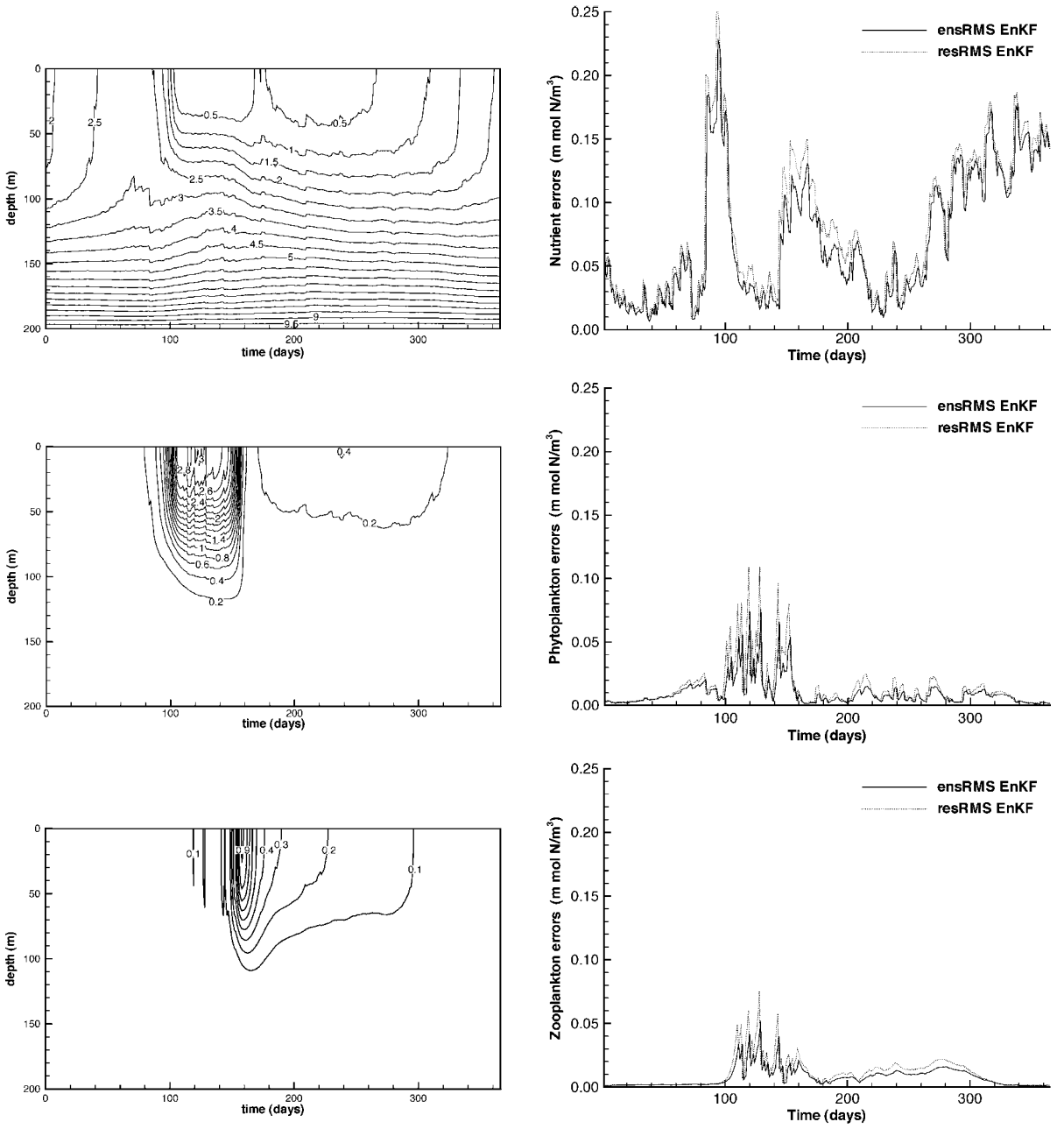

Fig. 5. Experiment 2 (Case 4C): The EnKF estimate (left plots) and comparison of the corresponding resRMS and ensRMS measures (right plots), for nutrient N (upper), phytoplankton P (center) and herbivorous zooplankton H (lower).

corrected until the next winter deepening and thus enhanced mixing of nutrients.

In general, the estimated root mean squares (ensRMSs), and the residual root mean squares (resRMS) are of similar magnitudes in Experiments 2 and 1. This is true for all the three ecosystem components, but it is especially notable for the concentrations of phytoplankton and zooplankton. An

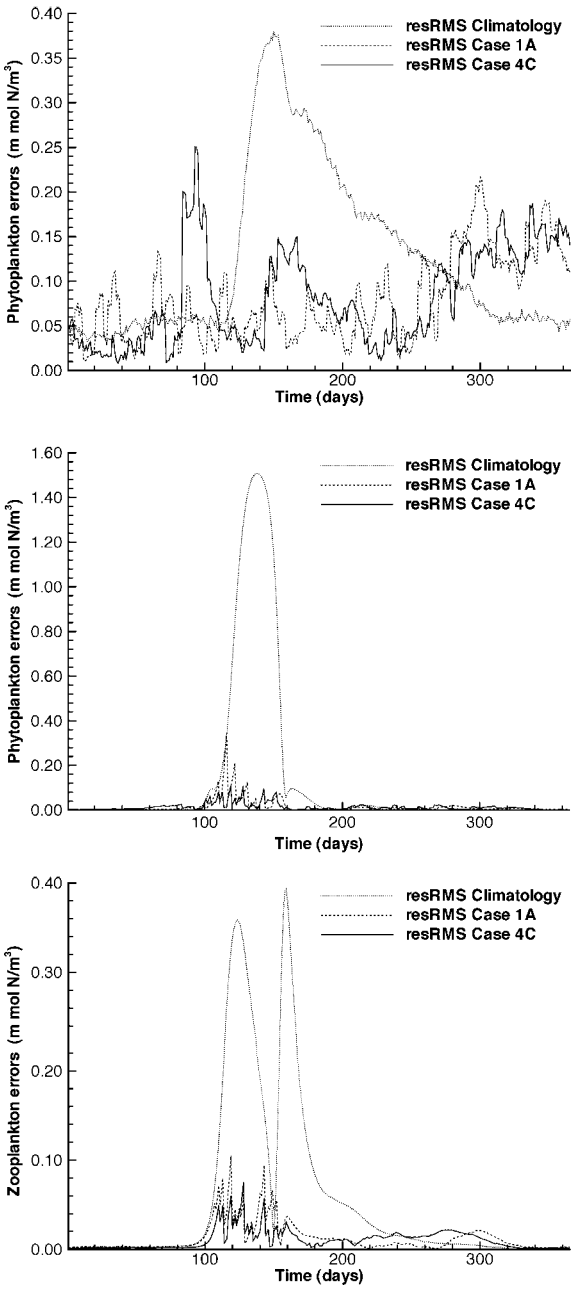

Fig. 6. Comparison of the resRMS values for the two main experiments and the climatology solution; nutrient N (upper), phytoplankton P (center) and zooplankton H (lower).

interesting point is the fact that the reduction of errors in the analysis step is significant for the unobserved zooplankton during the spring bloom. Thus, the result after the reduction is that the ensRMS and the resRMS are at about the same level as in Experiment 1 at the measurement locations. This shows that even if only the phytoplankton concentration has been measured, the statistical cross-correlations provided by the ensemble statistics are sufficient to update also the zooplankton concentration.

From the plots in Fig. 6, it is seen that the errors decrease every time observations are assimilated and are increasing in between the measurement times. The increase is caused by a combination of stochastic model errors and the internal nonlinear instabilities inherent in the model dynamics. In addition, the signal as well as the rate of change of the various concentrations are the strongest in this period. The stochastic model errors are accumulated in a linear fashion (although their effect evolves by the nonlinear equations). The internal instabilities are strongest during the spring bloom, where small perturbations will grow quickly (see Appendix B). In addition, the signal as well as the rate of change of the various concentrations are the strongest in this period. After the spring bloom, the dynamics are stabilizing and perturbations decrease, thus, errors are decreasing too. A linear stability analysis (see Appendix B) shows that the tangent linear operator has eigenvalues larger than one during the spring bloom and less than or equal to one elsewhere, and thus, the model is unstable in the spring bloom period but stable elsewhere. The strength of the EnKF is that it can handle these nonlinear and unstable regimes in a consistent way, and thus makes the method suitable for applications with models of this character, such as marine ecosystem models. This also shows that the measurements are mostly needed during the spring bloom where the instability is the strongest.

This will be further discussed and proven to be true, for our model and method, in the next section.

5. Sensitivity studies

In the following sections, the impact of varying the ensemble size, the number of measurements and prior error variances for the assimilation experiments will be studied. Experiments where observations of the nutrient concentration, N, only, and the zooplankton concentrations H, only, are assimilated, will also be

presented. Finally, the effect of using measurements from the bloom period, only, and from only the periods before and after the phytoplankton bloom will be presented. The same configuration as in Section 4 is used, and the errors in the boundaries and initial conditions are the same in all the experiments. However, the errors in the dynamics and measurements variy (see Table 3).

In all the plots concerning the varying variances in Section 5, the estimates of the concentrations of the three state variables at 20 m and the time series of the depth averaged residual root mean square (resRMS) are shown.

5.1. Impact of ensemble size

The size of the ensemble is important. If too few members are used, we will not be able to get the correct estimate of the error covariances in the predicted model state. Previous experience indicates that about 100 members are sufficient, but this has to be checked for every new model system (Evensen and van Leeuwen, 1996; Evensen and Fario, 1997; Houtekamer and Mitchell, 2001).

In Fig. 7, the relative difference between the concentration of phytoplankton in the respective cases, 1A, 1D, 1G and 1H, are shown. The difference at a certain time, has been calculated according to the formula

$$\mathrm{rel}P = \frac{P - P_{1\mathrm{H}}}{P_{1\mathrm{H}}}, \tag{9}$$

where P is the concentration of phytoplankton for the actual experiment and $P_{1\mathrm{H}}$ is the corresponding concentration in Case 1H. Thus, the difference between two cases has been normalized by the concentration of phytoplankton from Case 1H where the largest ensemble size (1000 members) was used. As may be seen from Fig. 7, the relative difference $\mathrm{rel}P_{1\mathrm{H}}$, is shown as the line $\mathrm{rel}P = 0$. When using 40 ensemble members, only, the amplitude of the errors is quite large and it contains many oscillations. Increasing the size of the ensemble to 100 results in errors, which are mainly within 10%, except from a few locations. The errors are only marginally smaller when the ensemble size is increased to 150. Thus, the improvement gained by using a larger ensemble than in Case 1A would only be marginal, and therefore, an ensemble of 100 members was chosen for our main experiments.

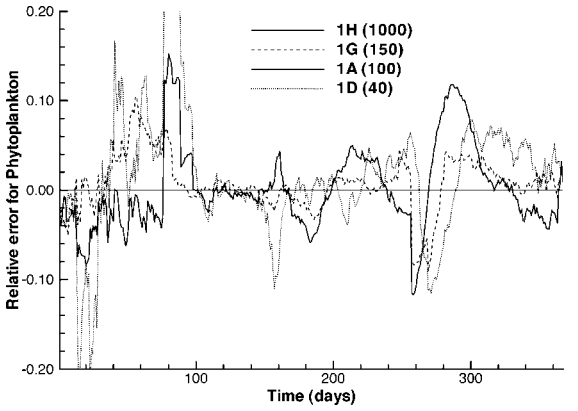

Fig. 7. Relative differences for phytoplankton concentration in cases using 1000, 150, 100 and 40 members in the ensemble, respectively. All the error variances were as in Experiment 1.

The theory behind the EnKF method implies that the accuracy of the representation of statistics in the EnKF should be proportional to $\frac{1}{\sqrt{\mathrm{nrsamp}}}$, where nrsamp is the number of ensemble members. The plot in Fig. 7 confirms that this is true for the experiments in this paper.

5.2. Definition of error variances

The errors in the measurements for ecosystem variables are roughly known. The errors in chlorophyll-*a* data obtained from Sea-viewing Wide Field-of-view Sensor (SeaWiFS) are said to be about 30–35% of the actual measurement value (Hooker et al., 1992). In situ data of the same measurement type contain slightly smaller errors (roughly about 20–30%). Measurements of zooplankton may contain large errors due to the rather unprecise net-towing technique used when measuring them. Since the pathways and parameters of ecosystems are not yet well known, the errors in the models available today may also be quite large. Another source of errors is the fact that the observations usually are defined in terms of chlorophyll-*a* while the model is defined in terms of phytoplankton nitrogen. Thus, a transformation between them has to be done and this may introduce new errors into the system.

The EnKF requires the specification of both the variances for the errors in the model and the errors in

the data. The choices of error variances affect the assimilation results. By choosing a small error variance for the observations, one assumes that the observations are fairly accurate and therefore only contain small errors. In such a case, the EnKF estimate will be close to the observations.

To ensure that the error bars of the observations and model estimates are statistically consistent, about 68.3% of the intervalls $[d-\sigma^d/d+\sigma^d]$ and $[m-\sigma^m/m+\sigma^m]$, where d, m, σ^m and σ^d are the observation, the model estimate, the standard deviation for the observation and the standard deviation for the model estimate, respectively, should be overlapping. This is true for a Gaussian distribution (Emery and Thomson, 2001). In other words, the prior assumption about the error statistics needs to reflect the true errors in the system. Otherwise, the predicted error variances will be erroneous and also the updates during the analysis may be suboptimal.

When studying the impact of different error variances in the measurements, we have used measurements of only one of the state variables. If more than one variable is assimilated, it becomes difficult to determine how much of the update is due to the direct measurements and how much is due to the multivariate covariances.

In Fig. 8, results for the nutrient concentration from Cases 3A to C (see Table 3) are shown. In these cases, observations of the concentration of nutrients, only, have been used in the assimilation. The sizes of the errors in the dynamics and the measurements are calculated as a certain percentage of the time and depth mean of the reference solution.

By comparing the two lower plots in the left column of Fig. 8, the effect of different error variances for the measurements may be observed. In the first experiment (the middle plot of the figure), the standard deviation of the errors in the observations is set to 1% (Case 3B in Table 3), while in the second experiment (the bottom plot of the figure) they have been increased to 30% (Case 3C in Table 3). The errors in the model have in both cases been set to 1%. It is easy to see that the EnKF estimate for the nutrients in the first experiment (middle plot) is much closer to the reference solution than in the second experiment (bottom plot). In the second experiment, there is hardly any impact of the observations at all when comparing with the climatology run. Our faith in the model compared to our faith in the data is much larger in this case than in the first.

By increasing the errors in the dynamics, the faith in the model is reduced and the result is an estimate which is closer to the observations. The relative impact of the observations has then been increased. In the leftmost upper plot of Fig. 8, results from an experiment, where the model errors are increased to about 3% while the measurement errors are still 1% (i.e. Case 3A in Table 3), are shown. From this plot, it is easy to observe that the EnKF estimate is closer to the observations than to the climatology. This is also reflected when comparing the plots in the right column of the figure. The resRMSs for the EnKF estimate of nutrients are the most reduced when the measurement errors are the smallest.

It is also obvious that the climatology estimate is further away from the reference solution in Case 3A than in the two other experiments shown in Fig. 8. This is due to the fact that by increasing the errors in the dynamics, the ensemble spreads more during the integration and the model estimate will deviate more from the reference solution. (Note that the climatology for different dynamical errors differ.)

Thus, the EnKF estimate is closer to the reference solution when the errors in the measurements are small and closer to the climatology, or pure ensemble run, when these errors were assumed large and/or if the dynamical errors are assumed small.

The effect on the variables that are not measured is discussed in Section 5.4.

5.3. Assimilation of all the three state variables in the model

Several experiments have been performed, observing all three model variables, with different magnitudes of model and measurement errors. The sizes of the dynamical and measurement errors are again given in Table 3. For all the experiments in this paper, a value called the depth and time averaged residual root mean square, referred to as the resRMStd, is calculated for each of the three state variables, N, P and H. This value is a measure of the distance between the reference solution and the EnKF estimate averaged over the depth–time domain, and it is used to check how well the EnKF does in tracking the reference solution in the different experiments performed.

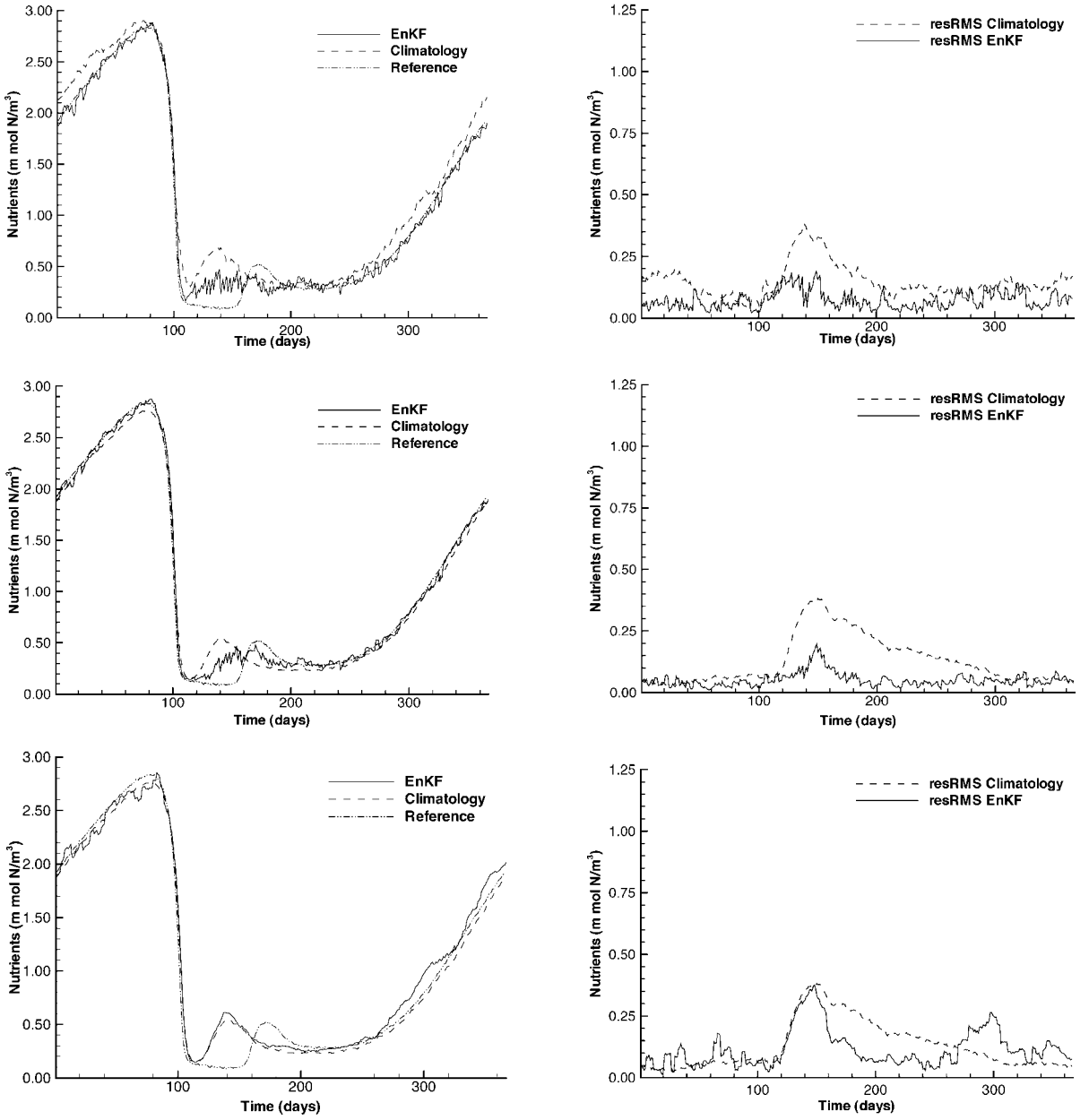

Fig. 8. The reference solution, climatology, the EnKF estimate at 20 m below the surface (left column) and the corresponding resRMS values (right column) for nutrients N in the Cases 3A (upper plots), 3B (middle plots) and 3C (bottom plots).

What may be observed from Table 3 is that the resRMStds are increased as the model, and/or measurement errors are increased (compare Case 2A with Cases 2B and 1A).

Note that the values in Table 3 only show results of one realization of the experiments. To compute statistically consistent resRMStds of such experiments, several repetitions of the same cases should have been

done with different random seeds and the average values of the resRMStds for these runs should be used.

5.4. Assimilation of one state variable, only

In the following, we present some experiments where measurements of only one of the state variables are assimilated. These experiments will provide information about the multivariate properties of the assimilation scheme, and about the controllability of the system, dependent of which variables are assimilated.

5.4.1. Assimilation of nutrient measurements

In Section 5.2, estimates and corresponding residual root mean squares (resRMSs), for the nutrient concentration for the Cases 3A–C, were shown. In this section, we will focus on the effect the assimilation of nutrients has on all the three state variables in the model.

When assimilating nutrients only, the updates of this variable is likely to be better than for the two others. All the state variables will, however, be influenced by the measurements through the multivariate properties of the assimilation scheme, which takes into account the estimated covariances between the different model variables.

In the upper plots of Fig. 8, results from Case 3A for all the three state variables are shown. As may be observed from this figure, the EnKF estimate for the nutrient concentration is reasonably good while the estimates of phytoplankton and zooplankton are only weakly updated and have values somewhere in between the climatology and the reference state. The errors are also the mostly reduced for the nutrients, as may be seen from the plots in the right column of the figure. Neither of the concentrations of phytoplankton and zooplankton reach the maximum value of the reference solution and they are both closer to the climatology than to the reference state.

When decreasing the errors in the model dynamics to 1%, as is done in Case 3B, the resRMStds for all the three state variables are reduced (see Table 3). This indicates that the EnKF for all the state variables is closer to the reference solution than in Case 3A, when averaging the distances between them over both depth and time. In the last experiment to be discussed in this section, the measurement errors are increased to about 30%. The model errors are still 1% (see Case 3C in Table 3). Compared to the resRMStds in Case 3B, the corresponding values, for the nutrients and phytoplankton, are increased. Even if the resRMStd for the zooplankton concentration is decreased, the sum of the resRMStds is increased. This implies that the EnKF estimate, as a total, is further away from the reference solution than in Case 3B. Anyway, the estimates for phytoplankton and zooplankton are not satisfactorily updated in any of the Cases 3A–C. In all the experiments discussed here, the bloom period comes too early, lasts too short and has a shape which is more similar to the climatology than to the reference state.

5.4.2. Assimilation of phytoplankton measurements

In this section, the experiments called Cases 4A–C in Table 3 are discussed. In these cases, observations of the phytoplankton concentration, only, are assimilated. The largest resRMStd for the nutrients is found when the dynamical errors are the largest, i.e. in Case 4B. For the zooplankton, however, the largest resRMStd is found in Case 4C where the measurement errors are large. Just as was the case for the experiments in the previous section, the sum of the resRMStds increases when the errors, either in the model dynamics or in the measurements, are increased.

In Fig. 9, results from Case 4A, for all the three state variables, are shown. The figure shows that the variable, which experiences the poorest update, is the nutrient concentration. This is true for all the cases in this section. However, even for this variable, the EnKF estimate is closer to the reference solution than to the climatology. The best result for the nutrients is found when the model errors are the smallest. Even when the measurement errors for the phytoplankton are 30%, the nutrient concentration is satisfactorily updated (see Experiment 2, Fig. 5). The zooplankton and phytoplankton concentrations are both well updated in all the three cases (see the resRMStds in Table 3). This shows that the influence from the phytoplankton measurements is larger on the zooplankton concentration than on the concentration of nutrients. The reason might be that the zooplankton and phytoplanton are stronger correlated than the phytoplankton and nutrients.

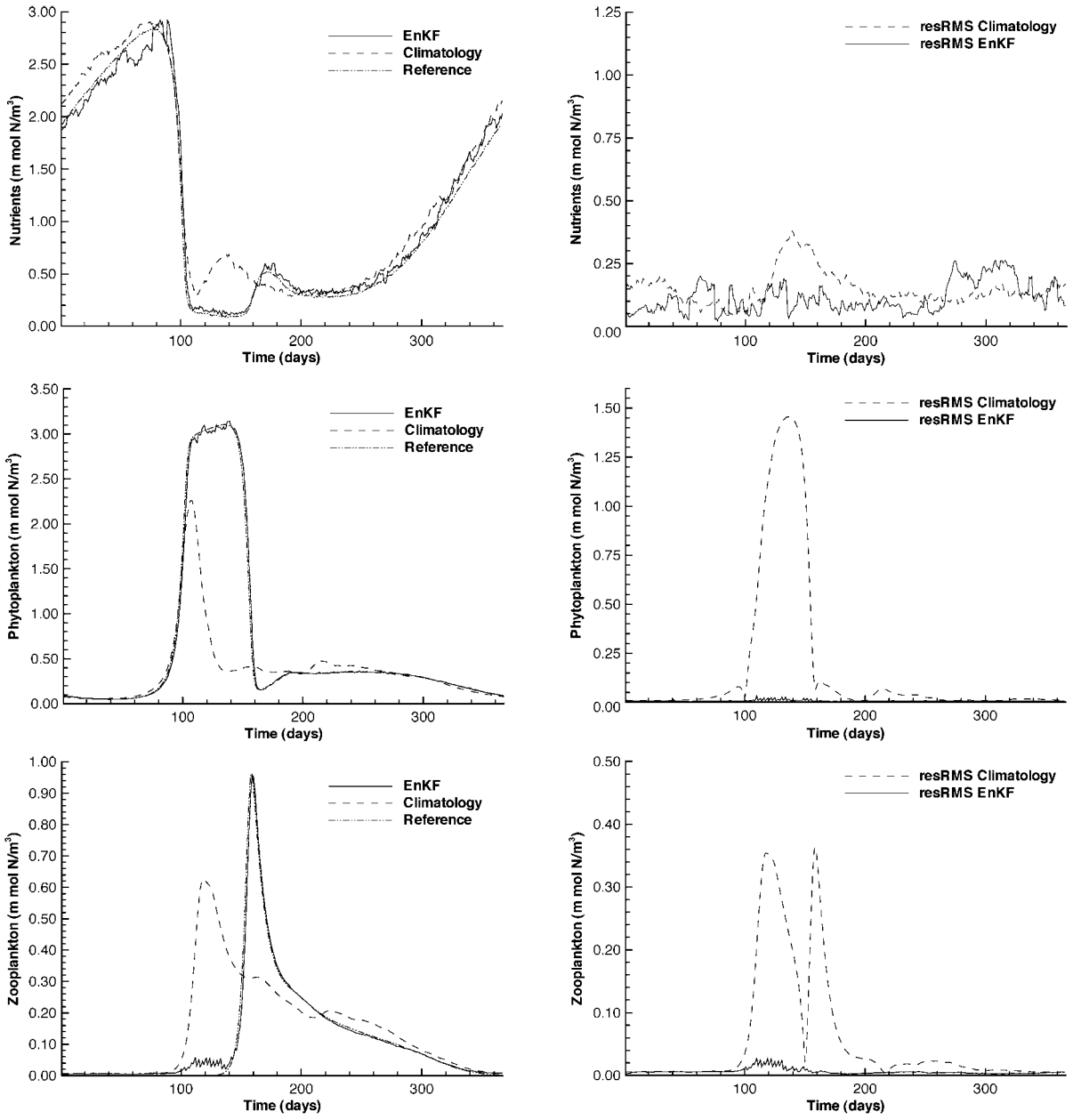

Fig. 9. Case 4A: The reference solution, climatology, the EnKF estimate at 20 m below the surface (left column) and the corresponding resRMS values (right column) for nutrient N (upper), phytoplankton P (center) and herbivorous zooplankton H (lower). Only observations of phytoplankton P have been assimilated and the errors were set to 1% for the measurements and 3% for the model dynamics.

Thus, it is possible to achieve good results by only using measurements of the concentration of phytoplankton with the EnKF technique and the simple 1-D model used in this paper.

5.4.3. Assimilation of zooplankton measurements

The experiments to be discussed in this section are the Cases named 5A–C in Table 3. In these cases, only observations of zooplankton are assimilated.

As may be noted, the percentages of errors are the same as in the cases in the two previous sections, and just as for those experiments, the sum of the resRMStds is increased when the errors in the dynamics and/or the measurements are increased. This is true even though the resRMStd for the nutrients is (slightly) decreased when the measurement errors are increased from 1% to 30% (Cases 5B and 5C).

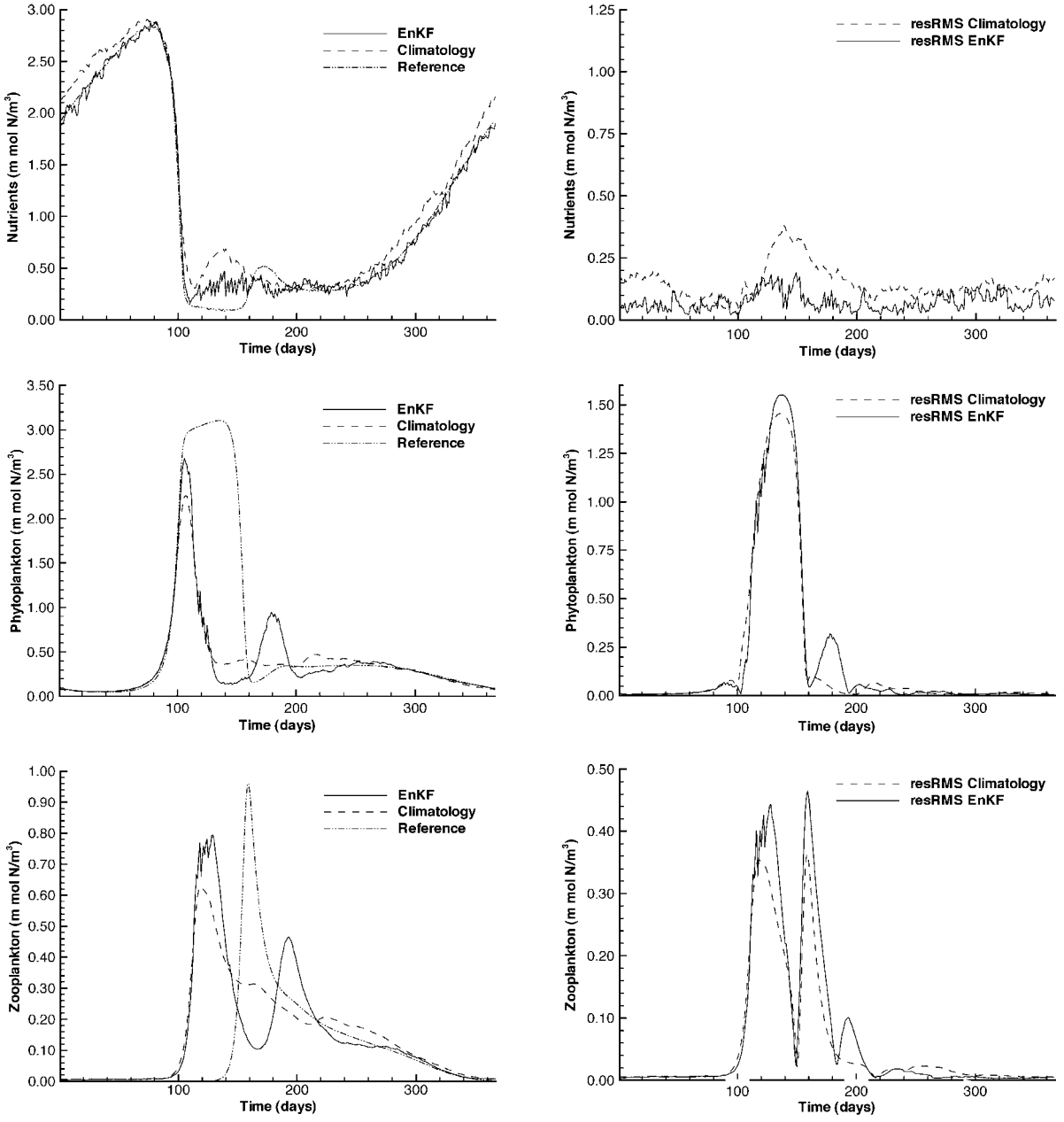

Fig. 10. Case 3A: The reference solution, climatology, the EnKF estimate at 20 m below the surface (left column) and the corresponding resRMS values (right column) for nutrient N (upper), phytoplankton P (center) and herbivorous zooplankton H (lower). Only observations of nutrients N have been assimilated and the errors were set to 1% for the measurements and 3% for the model dynamics.

Results from Case 5A are shown in Fig. 11. From this figure, it is obvious that the update of the nutrients is not as good as in the experiments in the previous section. It is especially poor from about days 40 to 90. However, some improvement is seen when the dynamical errors are the smallest, i.e. as in Cases 5B and 5C.

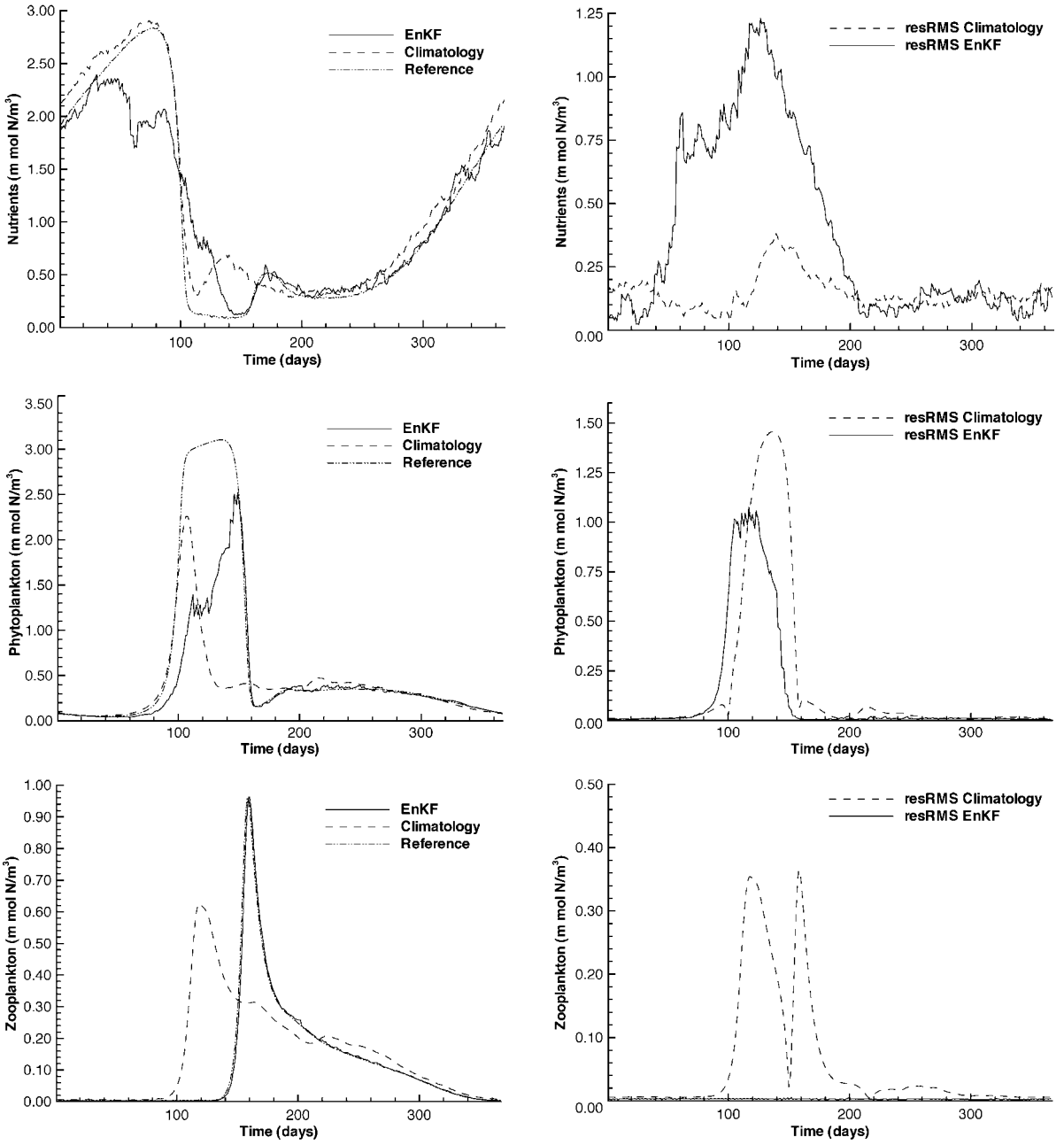

Fig. 11. Case 5A: The reference solution, climatology, the EnKF estimate at 20 m below the surface (left column) and the corresponding resRMS values (right column) for nutrient N (upper), phytoplankton P (center) and herbivorous zooplankton H (lower). Only observations of zooplankton H have been assimilated and the errors were set to 1% for the measurements and 3% for the model dynamics.

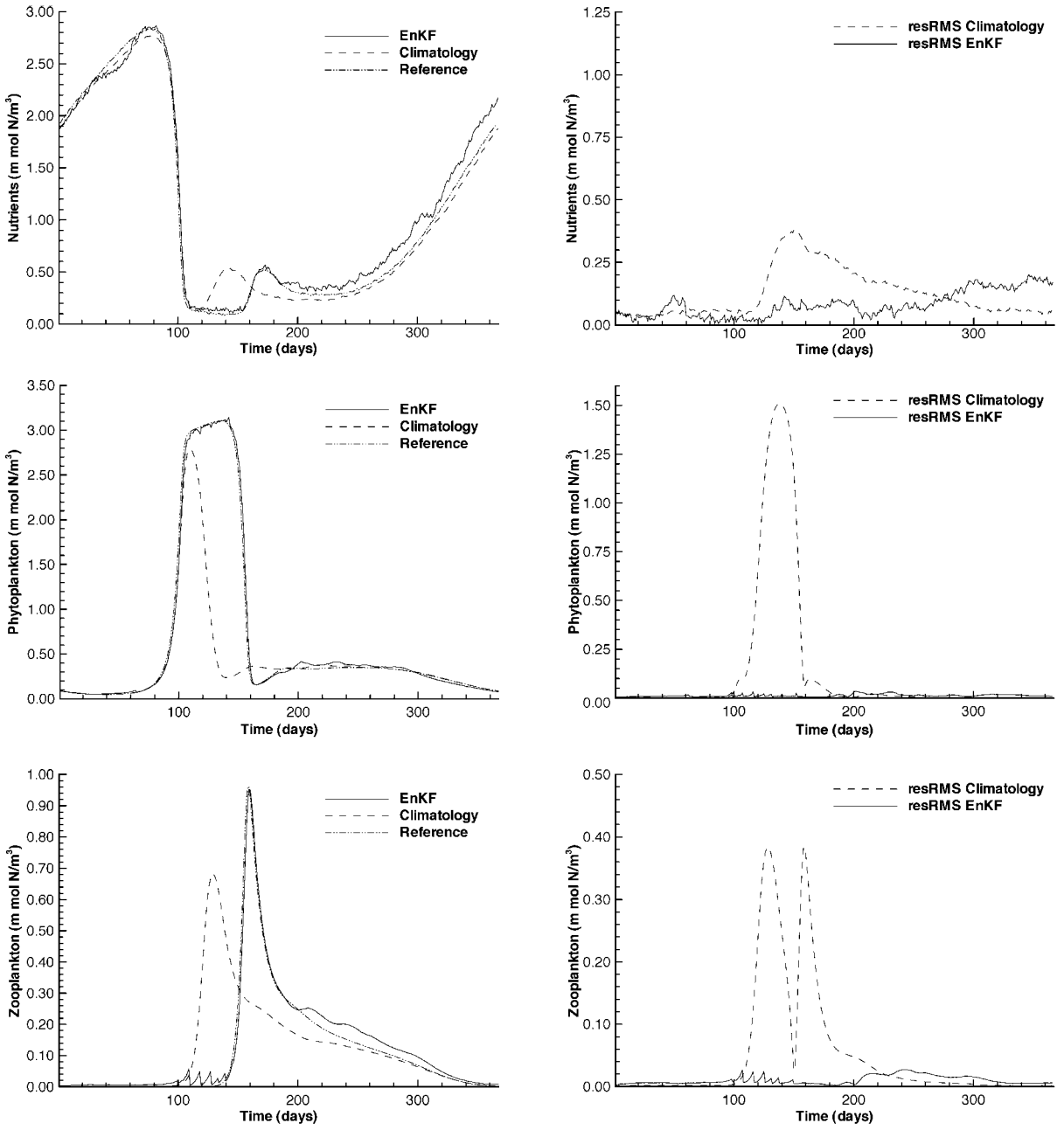

Fig. 12. Case 6B: The reference solution, climatology, the EnKF estimate at 20 m below the surface (left column) and the corresponding resRMS values (right column) for nutrient N (upper), phytoplankton P (center) and herbivorous zooplankton H (lower). Observations of all the three state variables have been assimilated, but only during the bloom period. The errors were set to 1% both for the measurements and the model dynamics.

The updates of the concentration of phytoplankton seem to be a bit better than they were seems to be stronger here than in the experiments in Section 5.4.1. The EnKF for this variable is closer to the reference solution for most of the time period (see the middle plots of Fig. 11) and the resRMStds are more reduced

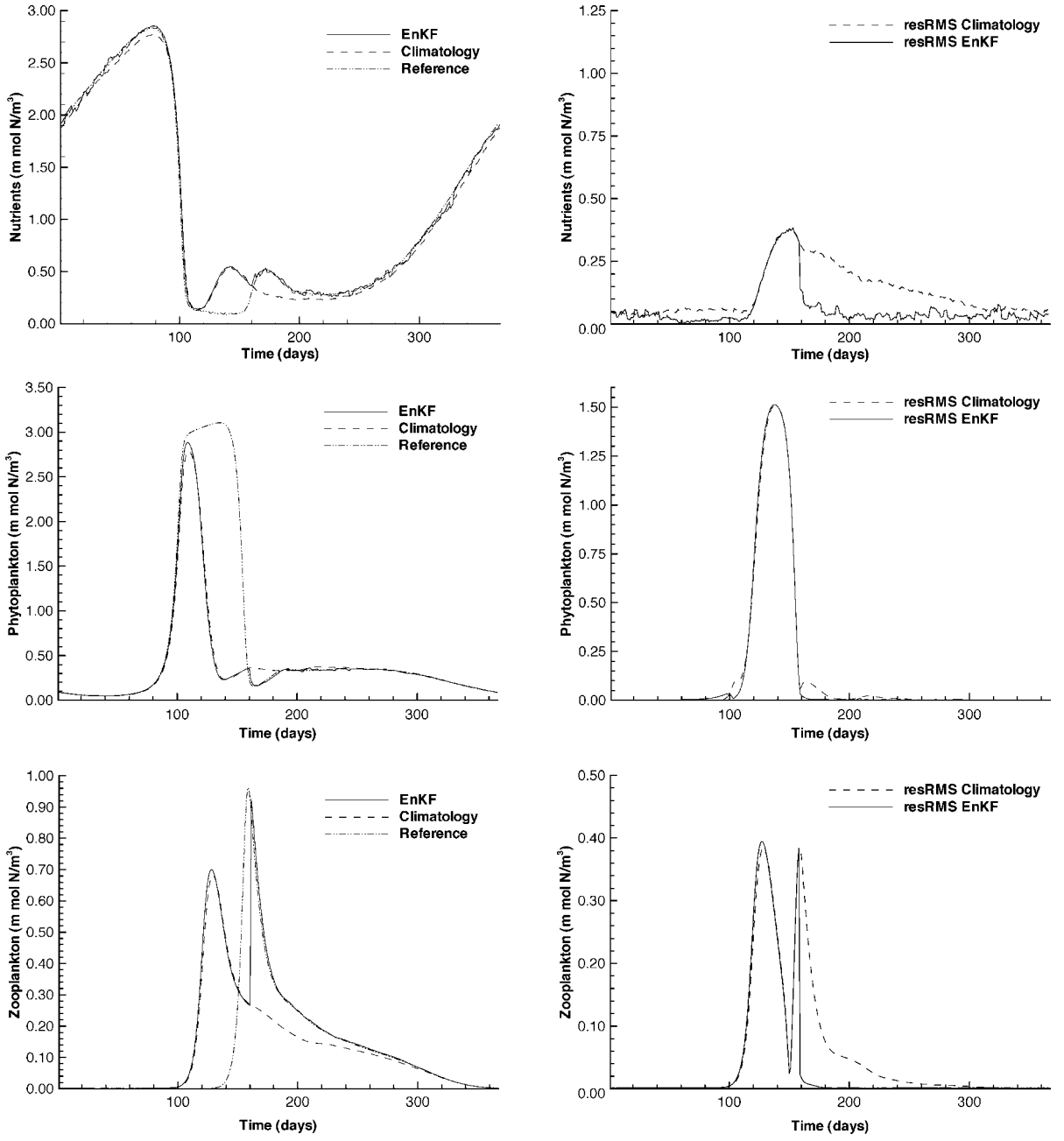

Fig. 13. Case 6A: The reference solution, climatology, the EnKF estimate at 20 m below the surface (left column) and the corresponding resRMS values (right column) for nutrient N (upper), phytoplankton P (center) and herbivorous zooplankton H (lower). Observations of all the three state variables have been assimilated, but only outside the bloom period. The errors were set to 1% both for the measurements and the model dynamics.

than in the experiments where only nutrients data were used (see Table 3).

Overall, the best result, for all the three state variables, is the one where the errors in the zooplankton measurements are the smallest and the model errors the smallest, i.e. the results from Case 5B (see the resRMStds in Table 3).

5.4.4. Summary

What has been seen in the previous sections is that in cases where only one state variable is measured and the measurement errors are allowed to be up to 30%, the results from the cases where phytoplankton data, only, were assimilated give the best result. The EnKF of the concentration of nutrients, which were the poorest update, was close to the reference solution through the whole year. The updates of the concentrations of phytoplankton and zooplankton almost fitted the reference solution perfectly at all times (see Fig. 9). In the experiments where measurements of only nutrients and zooplankton were used, assimilation results were far from as good (see Figs. 10 and 11).

Thus, the best result for all the three variables when measurements of one model variable, only, are used, is obtained when measurements of the concentration of phytoplankton are used. This may be caused by the fact that the phytoplankton is controlling much of the model evolution, by grazing on nutrients and being the prey for the zooplankton.

Note that the conclusion here is valid only for the NPZ model used in this study. If another model was used, the conclusions might change.

5.5. Assimilation of data from different time periods

In all the previous experiments, the residual root mean squares (resRMS's) are the largest in the spring bloom period, i.e. from about day 60 to about day 160. The changes in the model dynamics, especially for the phytoplankton and zooplankton, are also the most rapid during the start and end of this period (see, e.g. Fig. 8). Therefore, it is likely that data are mostly needed in this period to control the evolution of the model. In Fig. 12, results at 20 m from an experiment, referred to as Case 6B in Table 3, verify this. In this experiment, observations, from all the three state variables, were assimilated during the bloom period, only. By comparing the resRMStds from this experiments with the other experiments in this paper, one may see that the resRMStds are relatively small and from Fig. 12, it is easy to see that the EnKF does a good job in tracking all the three variables both during the bloom and elsewhere.

In Case 6A in Table 3, the resRMStds and the sizes of the errors used for an experiment with measurements from the time periods before and after the phytoplanktom spring bloom, only, are given. Plots of the EnKF estimate for this experiment are shown in Fig. 13. Here, the estimate is good outside the bloom period while it is unable to describe the bloom accurately. Thus, it seems to be more important to use measurements from the spring bloom period than from the rest of the year in order to achieve a good overall estimate.

This is no surprise. After all, it is in the spring bloom period, the models are the most unstable (see Appendix B) and the most rapid changes in the ecosystem take place. For the rest of the year, the model is stable, and thus, it will perform well for these periods even without, or with a few measurements only. Therefore, the main issue is to have data from the bloom period.

6. Summary

An Ensemble Kalman Filter has been used with a simple three-component marine ecosystem model which is a one-dimensional extension of the vertically integrated ecosystem model by Evans and Parslow (1985). First, two assimilation experiments are described, one where observations of all three model variables were assimilated and a second where only observations of the phytoplankton variable were assimilated. Both of these experiments show that the EnKF is capable of handling the nonlinear instabilities during the spring bloom, which is a critical issue when choosing a particular assimilation technique. The performance of the assimilation cases was also shown to significantly reduce the errors compared to a climatology simulation where no data were assimilated. Of particular interest is the result that even if only observations of the phytoplankton variable are assimilated, the assimilation system is capable of controlling the evolution of the whole model state including the zooplankton and the nutrients. This is a

capability of the EnKF, which provides a consistent multivariate analysis scheme based on the ensemble statistics which include the information about cross-correlations between different model variables. Thereafter, an extensive sensitivity analysis was presented. Here, it was concluded that an ensemble size of 100 seemed to be sufficient for the ensemble Kalman filter to converge. Further, the assimilation of nutrients only or zooplankton only provided less control over the model. The results in this paper give in our opinion an indication that the EnKF may become useful for applications where more sophisticated ecosystem models are used.

Acknowledgements

This work has been supported by the EC MAST-III BASYS project (MAS3-CT96-0058) and the EC MAST-III PIONEER project (MAS3-CT98-0170), and has received support from TRU through a grant of computer time.

Appendix A. Vertical dependence of photosynthetic light

As in Evans and Parslow (1985), formulas for photosynthetic light rate and the phytoplankton growth caused by light are assumed equivalent. However, while Evans and Parslow (1985) averaged it over the mixed layer depth, it is here calculated online at given depths where it is needed. Thus, the specific growth rate for phytoplankton averaged over a day at the depth, z, is now given by

$$\alpha(t,z,P) = 2Q^2 \frac{\tau}{\alpha_{\mathrm{II}} J} \mathrm{e}^{k_1 z_i} \left(\sqrt{1 + \frac{(\alpha_{\mathrm{II}} J)^2}{Q^2} \mathrm{e}^{-2k_1 z_i}} - 1 \right), \tag{10}$$

where $k_1 = k + l \int_0^z P(z',t)\mathrm{d}z'$. The parameters k, l and α_{II} are given in Table 4 and the light level at the surface at noon J, and the daylength 2τ are defined as in Evans and Parslow (1985). Note that in the expression above, α goes towards zero when the depth, z, goes to infinity.

Table 4
Physical light parameters, appropriate to Flemish Cap, identical to the ones used by Evans and Parslow (1985) in their first experiment

Symbol	Description	Value
k	Light attenuation by water	0.10 m^{-1}
l	Light attenuation by phytoplankton	0.12 m^2/mmol
b	Cloud cover	0.9
Q	Maximum photosynthetic rate	2 day^{-1}
α_{II}	Low light photosynthetic slope	0.04 m^2/W day
ϕ	Latitude	47°N

Appendix B. Stability analysis of the model

In this section, we perform a stability analysis (see Struble, 1962) of the model systems (1) systems (2) systems (3). Let $\phi^T(t,z)=(N(t,z), P(t,z), H(t,z))$ and $\boldsymbol{f}$ be defined as the right hand side of the equation (1) to (3), i.e.

$$\boldsymbol{f}(\phi(t,z)) = \begin{cases} -\left[\frac{\alpha_0 N}{j+N} - r\right] P \\ +\left[\frac{\alpha_0 N}{j+N} - r\right] P - \frac{c(P-P_0)H}{K+P-P_0}, \\ +\frac{fc(P-P_0)H}{K+P-P_0} - gH \end{cases} \tag{11}$$

where we have omitted the diffusion terms and assumed that the specific growth rate $\alpha(t,z,P)=\alpha_0$ is constant, to simplify the calculations. For simplicity, the diffusion term has been omitted in the further analysis, meaning that we are only considering the stability of the biological interactions in a local point, i.e. at a certain depth in our case.

Further, the constant α_0 only changes the light distribution with depth and should not alter the conclusions.

We can now write our model equation on the form

$$\frac{\partial \phi(t,z)}{\partial t} = \boldsymbol{f}(\phi(t,z)). \tag{12}$$

The stability characteristics, or eigenvalues, of a nonsingular trajectry $\phi(t,z)$ of such an equation are

reflected in the stability characteristics of a singular solution of a related equation. Let us assume that ϕ^* is a neighbouring solution of our equation, then the perturbation function $\eta(t,z)=\phi(t,z)-\phi^*(t,z)$ satisfies the perturbation equation

$$\frac{\partial \eta(t,z)}{\partial t} = \boldsymbol{f}(\phi(t,z)) - \boldsymbol{f}(\phi(t,z)-\eta(t,z)) = \boldsymbol{f}^*(\eta(t,z)), \tag{13}$$

where the right hand side vanishes for $\eta(t,z)=0$. (i.e. for $\phi=\phi^*$). Thus, ϕ is a stable solution of Eq. (12) if, and only if, the trivial solution, $\eta=0$ of Eq. (13) is stable.

For our model system, the perturbation equation is given by

$$\frac{\partial \eta}{\partial t} = \boldsymbol{A}(\phi)\eta, \tag{14}$$

where the matrix $\boldsymbol{A}$ is given by

$$\boldsymbol{A} = \begin{pmatrix} -\frac{\alpha_0 P}{(j+N)^2} & -\left[\frac{\alpha_0 N}{j+N} - r\right] & 0 \\ \frac{\alpha_0 P}{(j+N)^2} & \frac{\alpha_0 N}{j+N} - r - \frac{cKH}{(K+P-P_0)^2} & -\frac{c(P-P_0)}{K+P-P_0} \\ 0 & \frac{fcHK}{(K+P-P_0)^2} & \frac{fc(P-P_0)}{K+P-P_0} - g \end{pmatrix}. \tag{15}$$

Here, the terms quadratic in η_N, η_P and η_H have been neglected and the Taylor expansions

$$\frac{N}{j+N} = \frac{N}{j+N} + \eta_N \frac{j}{(j+N)^2} - \frac{(\eta_N)^2}{2!}\frac{2j}{(j+N)^3} + O((\eta_N)^3) \tag{16}$$

and

$$\frac{P-P_0}{K+P-P_0} = \frac{P-P_0}{K+P-P_0} + \eta_p \frac{K}{(K+P-P_0)^2} - \frac{(\eta_P)^2}{2!}\frac{2K}{(K+P-P_0)^3} + O((\eta_P)^3) \tag{17}$$

have been used.

The matrix $\boldsymbol{A}$, is called the tangent linear operator or the Jacobi matrix, $(\partial f_i/\partial \phi_j)$, of our original model.

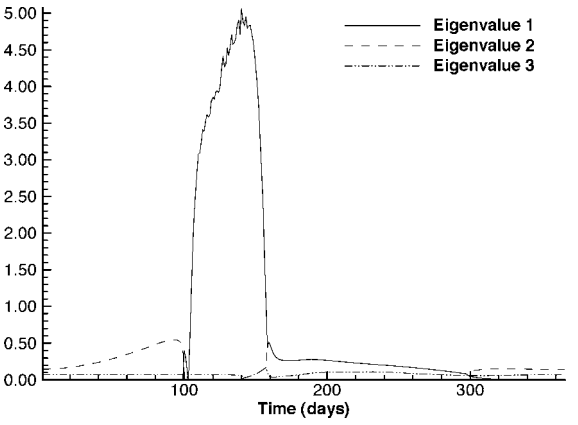

Fig. 14. The three eigenvalues of the linearized three-variable model system as a function of time.

Of course, $\boldsymbol{f}(\phi,t)$ has to be assumed continuously differentiable in ϕ.

Thus, to check the stability of our model systems (1) systems (2) systems (3), we need to calculate the stability characteristcs, i.e. the eigenvalues λ of $\boldsymbol{A}$. These are found by solving the system

$$\det(\lambda \boldsymbol{I} - \boldsymbol{A}) = 0, \tag{18}$$

where $\boldsymbol{A}$ is evaluated given the trajectory ϕ.

For a linear system, the eigenvalues will be constant in time. For a nonlinear system, like the one in this paper, the eigenvalues are functions of the state variables and thus dependent on time. The absolute values of the eigenvalues determine whether a system is stable or not. At times when $\lambda_{\max} \leq 1$, the model system is stable and at times when $\lambda_{\max} > 1$, the system is unstable.

The absolute values of the resulting three eigenvalues for our model is shown in Fig. 14. As may be observed, our system is stable in the period from day 0 to about day 100 and from day 160 to the end of the year, while it is unstable during the spring bloom period (days 100 to 160).

Appendix C. Stochastic forcing in the EnKF

In the EnKF, all the statistical information is represented by an ensemble of model states. The size of the ensemble is normally chosen large enough to

reduce the statistical fluctuations in the ensemble statistics to an acceptable level. The creation of the initial ensemble and the stochastic forcing used is based upon the use of psudo random statistical perturbations, see e.g. Evensen (1994) and Grønnevik and Evensen (2001).

A.1. Initial ensemble

Starting from a best guess model state $\bar{\psi}$, ensemble members are created by adding smooth pseudo random perturbations to $\bar{\psi}$

This is done using a formula which for nutrients $N(z)$, for member j, becomes

$$N_j(z) = \overline{N(z)}(1 + N_j'(z)\sqrt{\sigma_{\text{ini}}^2}) \tag{19}$$

where $N_j'(z)$ is a perturbation which is smooth in depth as determined by a specified covariance function. The ensemble of such perturbations has for each depth a normal distribution $N(0, 1)$. Thus, in the formula above, we are adding perturbations with variance equal to σ^2. A similar equation is used for the other ecosystem variables.

A.2. Model errors

The dynamical variance (stochastic model error) is incorporated into the model using the formula

$$N_j(z) = N_j(z)(1 + N_j'(z)\sqrt{\sigma_{\text{dyn}}^2}), \tag{20}$$

and the variances used in the different experiments are given in Table 3. It applies to the entire vector of state once every day during the forward integration.

A.3. Measurement errors

The ensemble of measurements is generated using the formula

$$d_j = \overline{d}(1 + \mu_j\sqrt{\sigma_{\text{obs}}^2}) \tag{21}$$

where μ_j is a random number taken from a Gaussian distribution with mean equal to zero and standard deviation equal to one. The standard deviation of the errors in the measurements used is given in Table 3.

References

Burgers, G., van Leeuwen, P.J., Evensen, G., 1998. Analysis scheme in the ensemble Kalman filter. Mon. Weather Rev. 126, 1719–1724.

Carmillet, V., Brankart, J.-M., Brasseur, P., Drange, H., Evensen, G., 2001. A singular evolutive extended Kalman filter to assimilate ocean color data in a coupled physical–biochemical model of the North Atlantic. Ocean Model. 3, 167–192.

Courtier, P., Talagrand, O., 1987. Variational assimilation of meteorological observations with the adjoint vorticity equation II: numerical results. Q. J. R. Meteorol. Soc. 113, 1329–1347.

Eknes, M., Evensen, G., 1997. Parameter estimation solving a weak constraint variational formulation for an ekman model. J. Geophys. Res. 102, 12479–12491.

Emery, J.E., Thomson, R.E., 2001. Data Analysis Methods in Physical Oceanography, 2nd rev. edn. Elsevier, Amsterdam, 638 pp.

Evans, G.T., Parslow, J.S., 1985. A model of annual plankton cycles. Biol. Oceanogr. 3, 327–347.

Evensen, G., 1992. Using the extended kalman filter with a multilayer quasi-geostrophic ocean model. J. Geophys. Res. 97 (C11), 17905–17924.

Evensen, G., 1994. Sequential data assimilation with a nonlinear quasi-geostrophic model using Monte Carlo methods to forecast error statistics. J. Geophys. Res. 99 (C5), 10143–10162.

Evensen, G., 1997. Advanced data assimilation for strongly nonlinear dynamics. Mon. Weather Rev. 125, 1342–1354.

Evensen, G., Fario, N., 1997. A weak constraint variational inverse for the Lorenz equations using substitution methods. J. Meteorol. Soc. Jpn. 75, 229–243.

Evensen, G., van Leeuwen, P.J., 1996. Assimilation of Geosat altimeter data for the Agulhas current using the Ensemble Kalman Filter with a Quasi-Geostrophic Model. Mon. Weather Rev. 124, 85–96.

Evensen, G., Dee, D., Schröter, J., 1998. Parameter estimation in dynamical models. In: Chassignet, E.P., Verron, J. (Eds.), Ocean Modeling and Parameterizations. Kluwer Academic Publishing, Netherlands, pp. 373–398.

Fasham, M.J.R., Evans, G.T., 1995. The use of optimization techniques to model marine ecosystem dynamics at the JGOFS station at 47°N 20°W. Trans. R. Soc. Lond., Ser. B 348, 203–209.

Grønnevik, R., Evensen, G., 2001. Application of ensemble-based techniques in fish stock assessment. SARSIA 86, 517–526.

Hooker, S.B., Esaias, W.E., Feldman, G.C., Gregg, W.W., McClain, C.R., 1992. An overview of SeaWiFS and ocean color. In: Hooker, S.B., Firestone, E.R. (Eds.), NASA Technical Memorandum 104566—SeaWiFS Technical Report Series, vol. 1. NASA.

Houtekamer, P.L., Mitchell, H.L., 2001. A sequential ensemble Kalman filter for atmospheric data assimilation. Mon. Weather Rev. 129, 123–137.

Hurtt, G.C., Armstrong, R.A., 1996. A pelagic ecosystem model calibrated with BATS data. Deep-Sea Res. II 43 (2–3), 653–683.

Ishizaka, J., 1993. Data assimilation for biogeochemical models. In: Ewans, G.T., Fasham, M.J.R. (Eds.), Towards a Model of Ocean Biochemical Processes. Springer-Verlag, Berlin, pp. 295–316.

Kalman, R.E., 1960. A new approach to linear filter and prediction problems. J. Basic Eng. 82, 35–45.

Kalman, R.E., Bucy, R.S., 1961. New results of linear filtering and prediction theory. J. Basic Eng. 83, 95–108.

Lawson, L.M., Spitz, Y.H., Hofmann, E.E., Long, R.B., 1995. A data assimilation technique applied to a predator–prey model. Bull. Math. Biol. 57 (4), 593–617.

Lawson, L.M., Hofmann, E.E., Spitz, Y.H., 1996. Time series sampling and data assimilation in a simple marine ecosystem model. Deep-Sea Res. II 43 (2–3), 625–651.

Matear, R.J., 1995. Parameter optimization and analysis of ecosystem models using simulated annealing: a case study at Station P. J. Mar. Res. 53, 571–607.

Miller, R.N., Ghil, M., Gauthiez, F., 1994. Advanced data assimilation in strongly nonlinear dynamical systems. J. Atmos. Sci. 51, 1037–1056.

Natvik, L.-J., Eknes, M., Evensen, G., 2001. A weak constraint inverse for a zero-dimensional four component marine ecosystem model. J. Mar. Syst. 28 (1–2), 19–44.

Navon, I.M., 1997. Practical and theoretical aspects of adjoint parameter estimation and identifiability in meteorology and oceanography. Dyn. Atmos. Ocean. 27, 55–79.

Prunet, P., Minster, J.-F., Echevin, V., Dadou, I., 1996a. Assimilation of surface data in a one-dimensional physical–biogeochemical model of the surface ocean: (2). Adjusting a simple trophic model to chlorophyll, temperature, nitrate and pCO_2 data. Global Biogeochem. Cycles 10 (1), 139–158.

Prunet, P., Minster, J.-F., Ruiz-Pino, D., Dadou, I., 1996b. Assimilation of surface data in a one-dimensional physical–biogeochemical model of the surface ocean: (1). Method and preliminary results. Global Biogeochem. Cycles 10 (1), 111–138.

Smedstad, O.M., O'Brien, J.J., 1991. Variational data assimilation and parameter estimation in an equatorial pacific ocean model. Prog. Oceanogr. 26, 179–241.

Spitz, Y.H., Moisan, J.R., Abbot, M.R., Richman, J.G., 1998. Data assimilation and a pelagic ecosystem model: parameterization using time series observations. J. Mar. Syst. 16, 51–68.

Struble, R.A., 1962. Nonlinear Differential Equations. McGraw-Hill, New York.

Talagrand, O., Courtier, P., 1987. Variational assimilation of meteorological observations with the adjoint vorticity equation I: theory. Q. J. R. Meteorol. Soc. 113, 1311–1328.

Yu, L., O'Brien, J.J., 1991. Variational estimation of the wind stress drag coefficient and the oceanic eddy viscosity profile. J. Phys. Oceanogr. 21, 709–719.

Yu, L., O'Brien, J.J., 1992. On the initial condition in parameter estimation. J. Phys. Oceanogr. 22, 1361–1364.